Tilted Transceiver Array for Ultra-high Field MRI

B. Wu[1], Y. Pang[1], C. Wang[1], D. Vigneron[1,2], and X. Zhang[1,2]
[1]Radiology&Biomedical Imaging, University of California, San Francisco, San Francisco, CA, United States, [2]UCSF/UC Berkeley Joint Group Program in Bioengineering, CA, United States

Introduction:

Ultra-high field transceiver coil array holds many advantages and unique capabilities over the conventional non-array volume transceiver coils such as B_1 shimming/manipulating and parallel excitation for human studies. The transceiver array can be either an array of loops or an array of straight microstrip elements [1-3]. Usually the mutual coupling in such arrays is minimized by using the dedicated decoupling network across the adjacent coil elements. The isolation better than -18dB, however, is technically challenging in practice. In addition, the depth of B_1 field may not be optimized due to the small gap between coil elements and the RF shield (or ground plane), although a ground plane benefits coil isolation and radiation loss reduction. The volume arrays with tilted microstrip and loop elements are proposed and investigated in this work. In those arrays, each element was tilted with a certain angle for achieving sufficient decoupling without using dedicated decoupling network. 8-ch human knee transceiver arrays with straight microstrips and loops were designed and tested at 7T. Decoupling is significantly improved for both arrays, and the B1 field is also increased in the imaging region for the microstrip array compared with non-tilted case.

Methods:

The receive-only venetian-blind array was introduced [4] for decoupling and G-map optimization. Our investigation shows that tilted elements are more useful for transceiver array decoupling since the element overlapping is not suggested and is extremely difficult to implement (microstrip). We built an 8-ch microstrip transceiver array and an 8-ch shielded loop transceiver array for human knee imaging (see Fig 1) using the tilted decoupling technique. Each microstrip element was built on a 1.2 cm thick Teflon board with the length of 16cm and width of 6cm. In the loop array, each loop is 16cm × 6cm, gap between the loop and the RF shield is 1.2cm. To conveniently adjust the tilted angle of each coil element (Fig 2), specific supporting frames were built with 21cm inner i.d. and 28 cm o.d. The isolation between two adjacent coil elements (unloaded case) was measured on bench with different angle θ. We also estimated the B_1 strength to tilted angles of a single loop/ microstrip element at the central point of the volume coil. We used a shielded pick-up coil to measure the induced voltages from two perpendicular directions. The combined voltage represented the B_1 field strength.

We simulated the B_1 distribution of the tilted microstrip array and the regular microstrip array (not tilted) at 300MHz with XFDTD (Remcom Inc.). To ignore the impact of mutual coupling, current sources with different phases (0°, 45°, 90°…) were placed at two ends of the eight elements. For fair comparison, the B_1 were finally normalized by dividing with the mean value of the background.

MR imaging experiments with the tilted microstrip array was performed on a 7T/90cm magnet. This scanner is equipped with two quadrature transmit channels and two T/R switches. To test the transceiver arrays on this system, continuous scans were conducted by connecting two coil elements into the transmit channels each time, and combined all sub-images offline. Phantom images and human knee images from a healthy volunteer were acquired with this array by using gradient echo (GRE) images. The acquisition parameters used were TE/TR= 6.9ms/100ms at 20°flip angle.

Results:

Bench measurements were shown in Fig 3. After tilting the microstrip elements with 30°, the best isolation of -22dB is observed. It is interesting that 28% more B_1 strength (efficiency) is also observed at the center point than that with $\theta = 0°$ (i.e. not tilted case). For the loop element, the best isolation occurs at 25°. With the 25° tilting, coil efficiency of the single loop dropped 10% than 0° case. After loading with a human knee, the coupling between adjacent elements in the regular microstrip array (not tilted) was relative strong (-10dB ~ -12dB). The isolation was improved to -19dB ~ -25dB after 30° element tilting. B1 fields from a single microstrip and a single loop are shown in Fig 4. Their different B1 field profiles further reveal their increase/decrease trends after the tilting. Fig 5 shows the simulated B_1^+ fields (unloaded case). With the similar B_1^+ strength at the periphery, the tilted array achieved >20% B_1^+ strength at the central part. Fig 6 shows the initial phantom and knee images acquired using the tilted microstrip array.

Conclusions:

Tilted transceiver microstrip and loop arrays have been demonstrated at 7T to achieve optimized isolation among resonant elements. For the microstrip array with tilted elements, B_1 strength is also increased at the depth. This array is particularly useful for large samples with densely-placed coil elements where element decoupling is usually problematic. The future investigation on this design will focus on the parallel imaging performance, safety issues, and the coil efficiency of the tilted transceiver array.

Acknowledgments:

This work was supported by NIH grants EB004453 UC Discovery ITLbio04-10148 and QB3 opportunity award. The authors would like to thank Dr. Eddy Boskamp for his valuable suggestions on this work.

References: [1] E. Boskamp et al. ISMRM 16th 2008 pp1094 [2] E. Boskamp et al. ISMRM 15th 2007 pp1046 [3] G. Adriany, et al. MRM 53, 2005, p434-445. [4] C. J. Hardy et al. ISMRM 13th 2005 pp 677

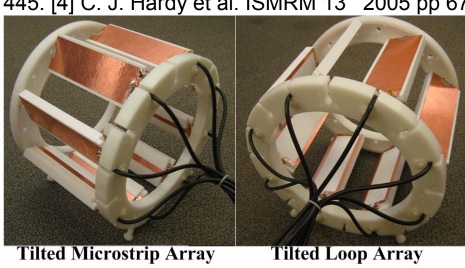

Tilted Microstrip Array **Tilted Loop Array**

Fig. 1 photos of tilted transceiver arrays

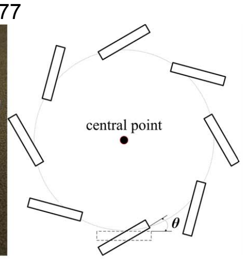

Fig. 2 Definition of tilted angle

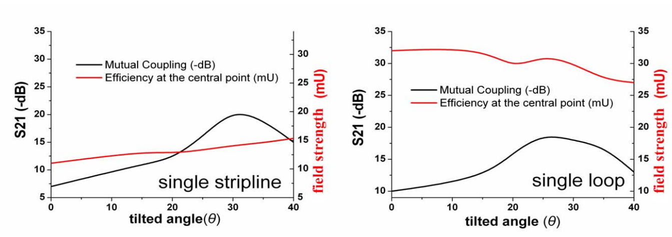

Fig. 3 Bench measurement of the decoupling/ field strength at central point of microstrip and loop elements

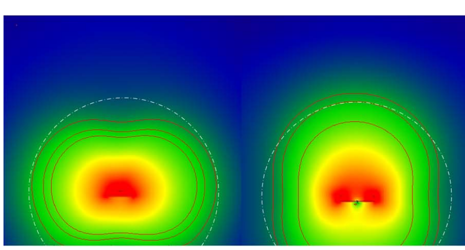

Single Microstrip **Single Loop**

Fig. 4 B1 field distribution of single microstirp and loop elements

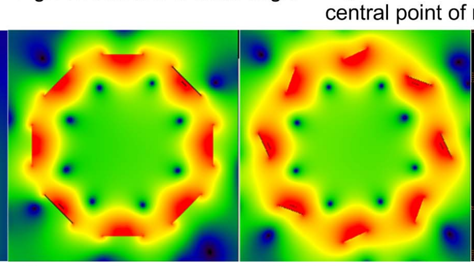

Regular Microstrip Array **Tilted Microstrip Array**

Fig. 5 $B1^+$ of tilted microstrip and loop arrays without loading

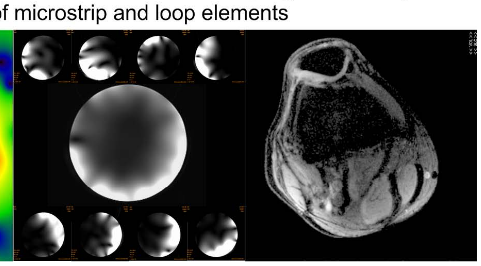

Fig. 6 Phantom and human knee images acquired with 8-ch tilted microstrip array at 7T